

WISCI

UNIVERSITY OF WISCONSIN • MADISON, WISCONSIN

PLASMA PHYSICS

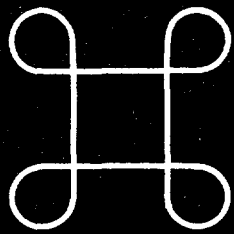
48
8-4-95 JS②

HIGH CURRENT PLASMA ELECTRON EMITTER

G. Fiksel, A.F. Almagri, D. Craig, M. Iida*,
S.C. Prager, and J.S. Sarff

DOE/ER/53198-261

July 1995



WISCONSIN

NOTICE

This report was prepared as an account of work sponsored by an agency of the United States Government. Neither the United States nor any agency thereof, nor any of their employees, makes any warranty, expressed or implied, or assumes any legal liability or responsibility for any third party's use or the results of such use of any information, apparatus, product or process disclosed in this report, or represents that its use by such third party would not infringe privately owned rights.

Printed in the United States of America
Available from
National Technical Information Service
U.S. Department of Commerce
5285 Port Royal Road
Springfield, VA 22161

NTIS Price codes
Printed copy: A02
Microfiche copy: A01

DISCLAIMER

This report was prepared as an account of work sponsored by an agency of the United States Government. Neither the United States Government nor any agency thereof, nor any of their employees, makes any warranty, express or implied, or assumes any legal liability or responsibility for the accuracy, completeness, or usefulness of any information, apparatus, product, or process disclosed, or represents that its use would not infringe privately owned rights. Reference herein to any specific commercial product, process, or service by trade name, trademark, manufacturer, or otherwise does not necessarily constitute or imply its endorsement, recommendation, or favoring by the United States Government or any agency thereof. The views and opinions of authors expressed herein do not necessarily state or reflect those of the United States Government or any agency thereof.

DISCLAIMER

**Portions of this document may be illegible
in electronic image products. Images are
produced from the best available original
document.**

High Current Plasma Electron Emitter

G. Fiksel, A.F. Almagri, D. Craig, M. Iida*, S.C. Prager, and J.S. Sarff

Department of Physics, University of Wisconsin at Madison, WI 53706, USA

*Kyoto Institute of Technology, Matsugasaki Sakyoky, Kyoto 606, Japan

Abstract

A high current plasma electron emitter based on a miniature plasma source has been developed. The emitting plasma is created by a pulsed high current gas discharge. The electron emission current is 1 kA at 300 V at the pulse duration of 10 ms. The prototype injector described in this paper will be used for a 20 kA electrostatic current injection experiment in the Madison Symmetric Torus (MST) reversed-field pinch. The source will be replicated in order to attain this total current requirement. The source has a simple design and has proven very reliable in operation. A high emission current, small size (3.7 cm in diameter), and low impurity generation make the source suitable for a variety of fusion and technological applications.

MASTER

DISTRIBUTION OF THIS DOCUMENT IS UNLIMITED

[Signature]

1. Introduction

A variety of technological and fusion applications demand a high current, efficient electron injector. The spectrum of technological applications is very broad, including plasma sources, ion and electron beams, plasma processing, etc. Electrostatic current injection has been used in fusion plasmas, usually on a small scale, for many years. For example, low current tokamak plasmas have been produced and sustained by electrostatic injection (often called dc helicity injection),¹ H-mode plasmas have been produced with biased electrodes², impurity generation has been controlled by biased electrodes,³ and plasma flow has been channeled by $\mathbf{E} \times \mathbf{B}$ effects induced by divertor plate biasing.⁴

The plasma injector described in this paper was created for a specific task requiring current injection in the Madison Symmetric Torus⁵ (MST) reversed field pinch (RFP) for the suppression of tearing instabilities and reduction of transport through a modification of the plasma current profile.⁶ The injected current could reduce the current density gradient which drives the fluctuations which are known to produce transport.^{7,8} Nevertheless, the source appears to be very versatile with a scope of applications far beyond these specific studies.

The common source of injected current is a biased electrode, usually either metal or hot (thermo-emissive) lanthanum hexaboride. Two dominant disadvantages of these techniques are that (1) the presence of biased material surfaces gives rise to strong plasma-electrode interactions with consequent impurity generation and reflux, and (2) the emitted current density is limited by material thermionic emission properties. In addition, during experiments with these types of electrodes in MST we discovered that

the emitted current does not exhibit the directionality required for current profile control.

We have proposed and tested a different kind of current injector that alleviates these problems. The key feature of the injector is that electrons are extracted from a miniature plasma source, rather than from an emissive material surface. The result is a source with low impurity generation, high current density, and effective direction control in comparison to typical metal electrodes. In this paper we present a detailed description of a prototype 1 kA electron injector. The source is described in Section 2, injector optimization studies in Section 3, and an optimized current injector for MST application in Section 4. This 1 kA injector will be replicated to implement a full scale 20 kA current injection system for current profile control studies in MST.

2. Plasma Source.

Various types of plasma cathodes have been studied^{9,10} for ion and electron beam applications. There are commercial products available that can be adjusted for various needs; for example, Spectra-Mat, Inc., CA¹¹ manufactures electron and ion injectors based on hollow cathode plasma sources with the total electron emission current ~ 10 A. For our specific requirements, among which are high per-unit emission current (~ 1 kA) and compatibility with fusion research grade plasmas we had to design a novel plasma electron injector.

The schematic of the injector is shown in Fig. 1. The injector contains a miniature plasma source in which a cylindrical, hydrogen, arc plasma is produced.^{12,13,14} A stack of molybdenum washers 1.5 cm - 2 cm tall with the inner diameter 0.6 cm - 1.0 cm defines the arc channel between an anode and cathode which are also molybdenum. The washers are isolated from each

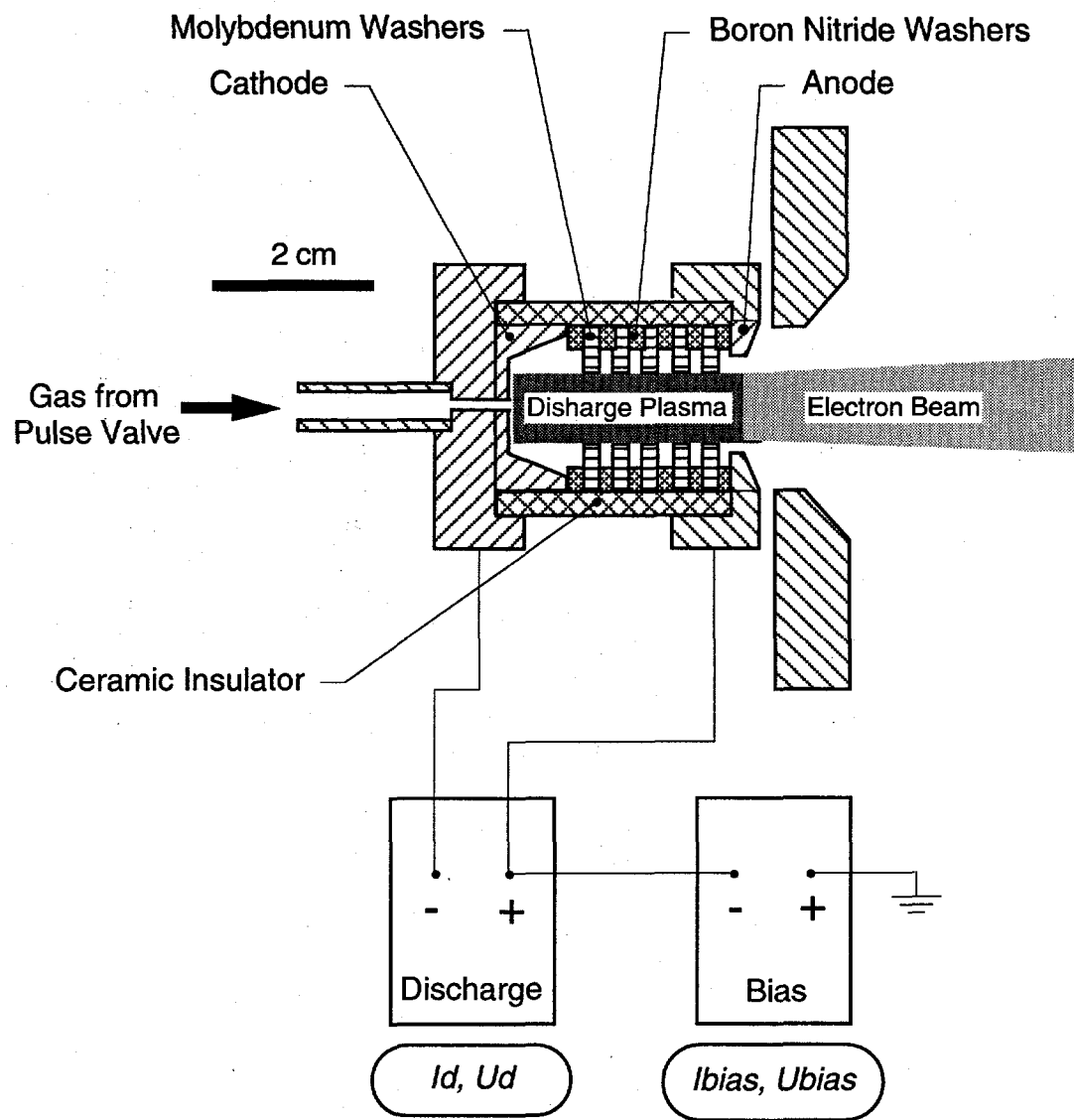


Fig. 1. Schematic of the plasma current injector - "straight" configuration.

other by 1 mm thick boron nitride washers. Gas is supplied through the cathode with a pulsed electromagnetic valve, and the arc plasma is maintained by a pulse forming network. The discharge voltage is about 80-100 V, and the discharge current can be varied from 0.5 kA to 3 kA. The plasma density measured at the source¹⁴ exit is $n \approx (1-3) \times 10^{14} \text{ cm}^{-3}$ and the electron temperature is $T_e \approx 10-20 \text{ eV}$. The discharge duration can be varied up to 10 ms depending on the power supply. The plasma source can operate without a magnetic field, although an axial magnetic field greatly improves the source efficiency.

Electrons are extracted from the source through the anode by biasing the anode (and therefore the source plasma) relative to the vacuum vessel wall or another object, e.g.. an electrode or another plasma-based injector.

We want to emphasize the fact that this plasma source design provides the user with a very high degree of flexibility in adjusting the source geometry to fulfill specific needs. The plasma chamber geometry is easy to modify, a feature which we exploited in our optimization experiments. The arrangement and the material of supporting isolators, configuration of current carrying electrodes, etc. can be varied significantly while retaining the cylindrical washer-stack discharge chamber geometry and without affecting the physical properties of the plasma. An example of a different configuration of the plasma source is shown in Fig. 2. While being identical in the geometry of the plasma chamber, these two configurations differ in the shape of the source. We used these two configurations in different experimental setups. The first configuration - "straight", utilizing the axial geometry of the magnetic field and the stand vacuum vessel, was mainly used in our optimization experiments in the test stand. The second configuration - "angled" is used for the current injection in MST. The plasma source is

inserted radially through a machine port and can be rotated to inject either poloidal or toroidal current. Incidentally, the "straight" configuration can be used in experiments for which radial injection is needed.

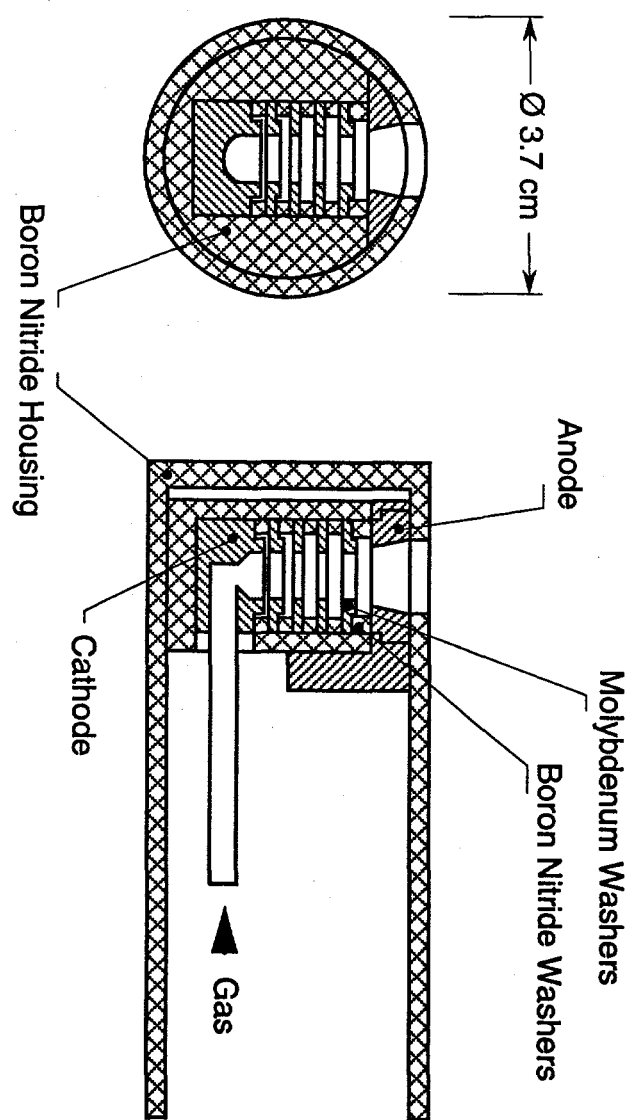


Fig. 2. Schematic of the plasma current injector - "angled" configuration. This figure also represents the MST current injector.

3. Injector Optimization Studies.

We have performed source optimization studies in order to evaluate and to minimize the gas throughput and to maximize the injection current. The "straight" gun was used in these experiments. The variable parameters in the experiment were the discharge chamber dimensions. Three gun configurations were tested with the parameters shown in Table I.

Table I. List of parameters for three plasma gun configurations.

Configuration	I	II	III
Discharge channel length (cm)	3.0	3.0	1.7
Discharge channel diameter (cm)	1.0	0.6	0.6

The experimental test stand setup with pertinent diagnostics and power supplies is shown in Fig. 3. The plasma source was attached to a vacuum vessel with a volume of $V_{ves} = 10^5 \text{ cm}^3$. The source was immersed in a 0.1 T magnetic field created by a set of Helmholtz coils. The magnetic field was uniform in the source region and diverging farther in the vessel. The gun was isolated from the vessel with a Plexiglas flange and was biased with respect to the vessel.

The injected beam current I_{beam} was measured with a beam monitor formed by a Rogowski coil embracing the beam. The beam current density J_{beam} profile was measured by a miniature movable Rogowski coil located 60 cm from the source. The gas density in the vessel was measured by an absolutely calibrated fast ion gauge. The plasma flow generated by the source was measured with a movable ion collector. In addition, we monitored the

discharge voltage U_d , discharge current I_d , bias voltage U_{bias} , and bias circuit current I_{bias} .

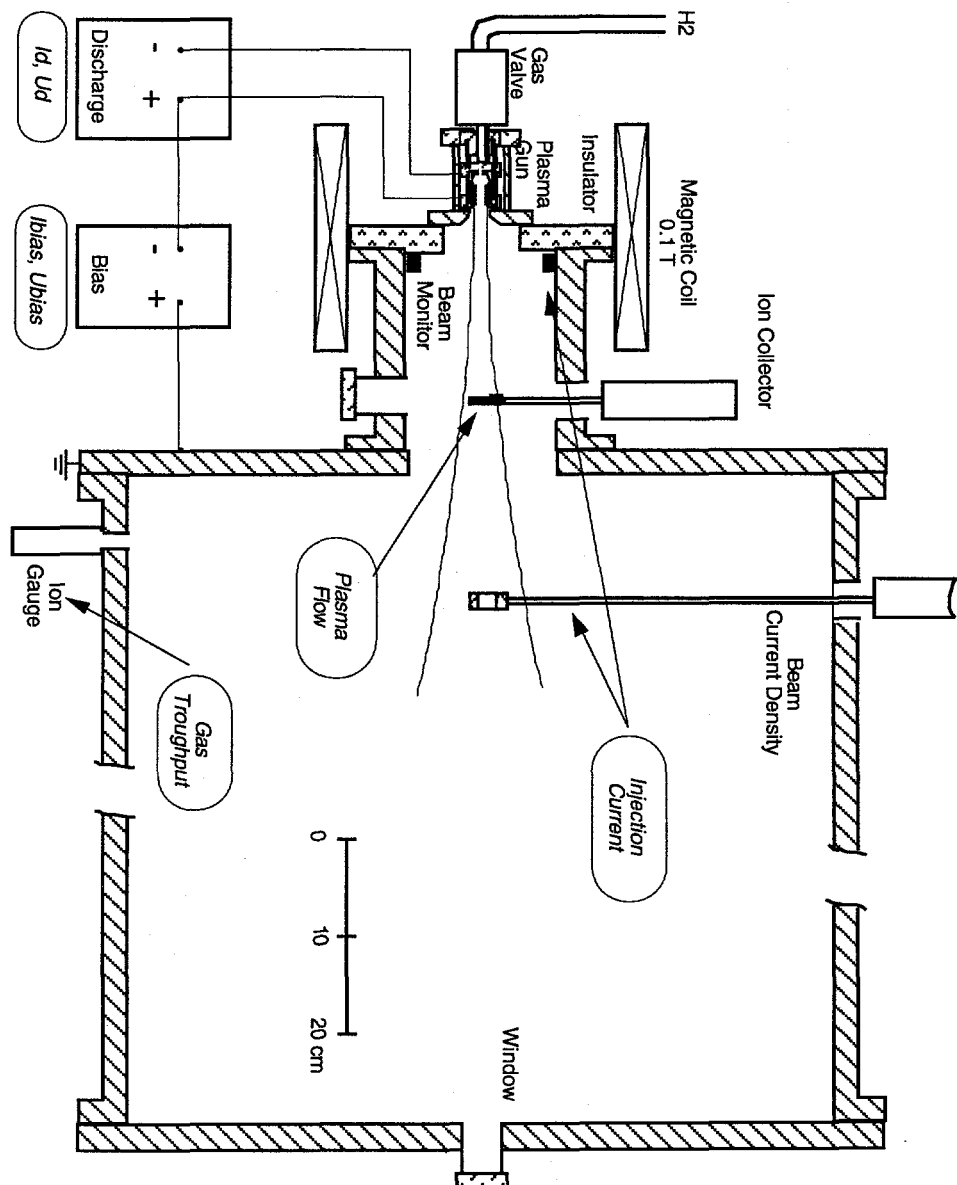


Fig. 3. Test stand - experimental setup, diagnostics and their functions.

The waveforms of the discharge current I_d and the gas throughput rate I_{gas} for the pulse duration of 2.5 ms are shown in Fig. 4. The gas rate in equivalent Amps was calculated using

$$I_{gas} = 2eV_{ves} \frac{dN_{H_2}}{dt}$$

where N_{H_2} is the hydrogen neutral density (pressure) in the vessel measured by the fast ion gauge and e is the electron charge. We include the factor 2 in order to estimate the gas utilization when compared to the H^+ ion flow from the gun. The gas rate was adjusted by changing the gas pressure in the valve.

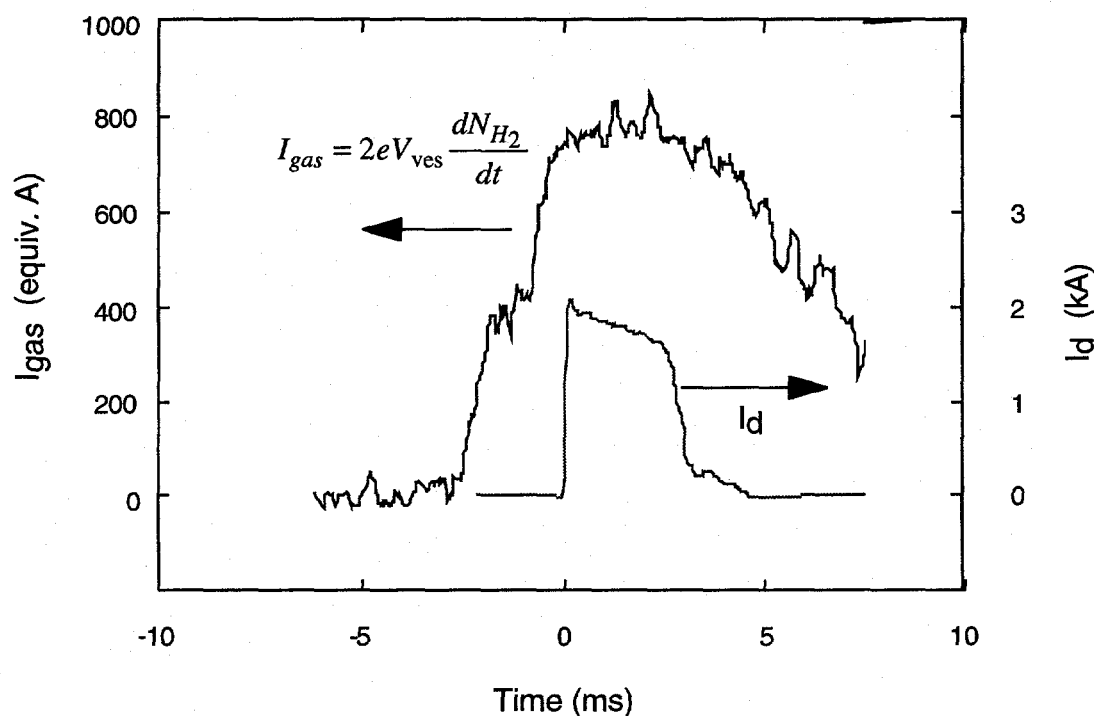


Fig. 4. Waveforms of the plasma source discharge current and gas throughput rate.

In order to measure the gas efficiency of the source we varied the discharge current at a given gas throughput rate and measured the ion current density J_i in the plasma flow. We also monitored the discharge voltage as an operational parameter of the discharge. We then repeated this for different throughput rates and the results for gun type I are shown in Fig. 5. For other configurations the results are similar.

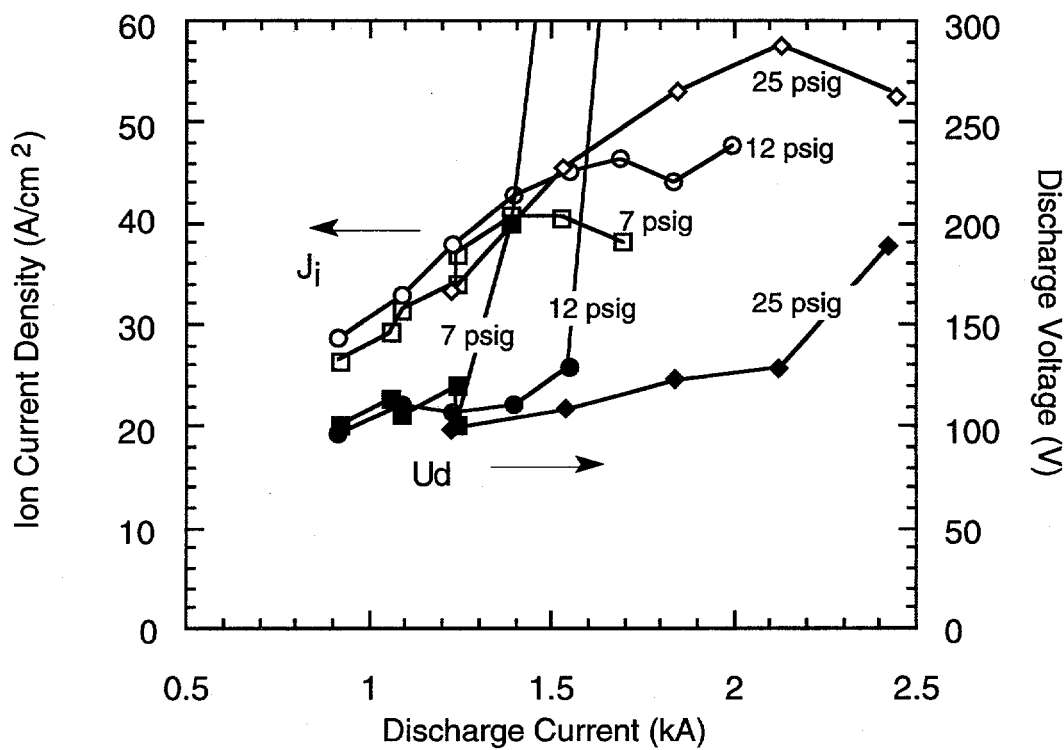


Fig. 5. Measurements of gas efficiency. Plasma flow ion current density (J) and the discharge voltage (U_d) vs. discharge current (I_d) at different valve pressures (throughput rates). The gas valve pressure in psig is indicated on the curves.

We see that for a given gas throughput rate there is an inflection point on the discharge voltage curve that corresponds to the maximum plasma production at a given throughput rate. Beyond that point the discharge voltage is increasing sharply over the nominal 90-100 V and plasma

production remains constant or even decreases. Below the inflection point the plasma production does not depend on the gas throughput and is proportional to the discharge current. Thus, this point corresponds to a maximum in the efficiency of the plasma source. The dependence of I_{gas} on I_d measured at this point is shown in Fig. 6 for different gun types. Under the optimized conditions the spatially integrated ion current density profile yielding the total ion flow $I_i \approx 0.1 \times I_d$ and $I_i \approx 0.3 \times I_{\text{gas}}$. Note that during the pulse the gas outflow from the source can be significantly lower to a high ionization ability of the plasma.

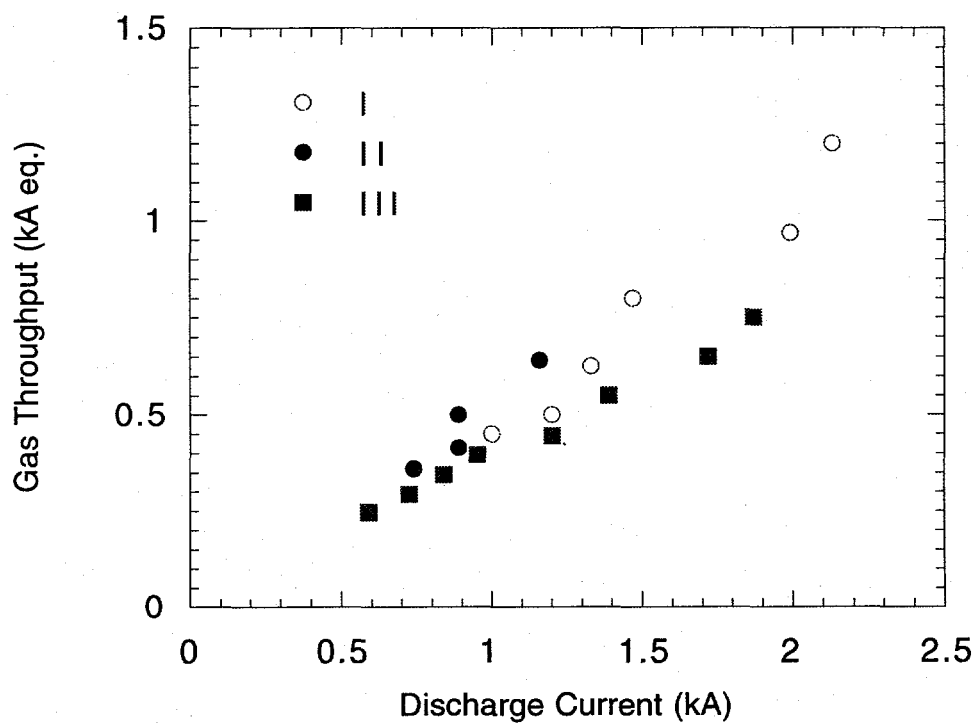


Fig. 6. The minimum gas throughput rate I_{gas} vs. the discharge current I_d . The gun configuration is indicated in the figure. The configuration size: I - 1 cm \times 3 cm, II - 0.6 cm \times 3 cm, III - 0.6 cm \times 1.7 cm.

When a bias voltage is applied the injected current flows along the magnetic field lines. The current is space charge neutralized due to the outgoing plasma, so the injector can be used for injection in vacuum as well as into other plasmas. The dependence of the injected current I_{beam} on the bias voltage U_{bias} at the discharge current $I_d = 1 \text{ kA}$ is shown in Fig. 7. We have found that there are two regimes of the injection differentiated by the relative steady-state amplitudes of the discharge current I_d and the beam current I_{beam} . These regimes are illustrated in Fig. 8 for $I_d = 1.2 \text{ kA}$. When $I_{\text{beam}} \leq I_d$, the waveforms of the total beam current and beam current density are identical to each other and to that of the discharge current - Fig. 8(b). The spatially integrated current profile is equal to the total beam current I_{beam} and to the bias circuit current I_{bias} . When $I_{\text{beam}} > I_d$, the waveform of the beam current becomes irregular Fig. 8(c) and the current profile widens. At the same time distinct arcing activity is observed on the anode surface. We identify the arcing activity by visible bright sparks on the surface and an increase in the H_α signal as monitored through a window opposite the gun. The results are similar for all gun configurations tested.

The fact that the maximum regular waveform injected current from the source is equal to the discharge current implies that in this case we divert all the discharge electrons in the source that otherwise would be collected on the anode and return them in the circuit through the injected current. When the injected current exceeds this limit, the extra electrons come through the arcing on the anode surfaces which is accompanied by broadening of the beam profile and irregular waveforms. In addition, the impurities generated by the arcing on the anode would contaminate the target plasma.

To summarize, we consider the optimum operational regime to be that in which the extracted current I_{beam} is equal to the discharge current I_d and the gas throughput rate is minimized according to Fig. 6.

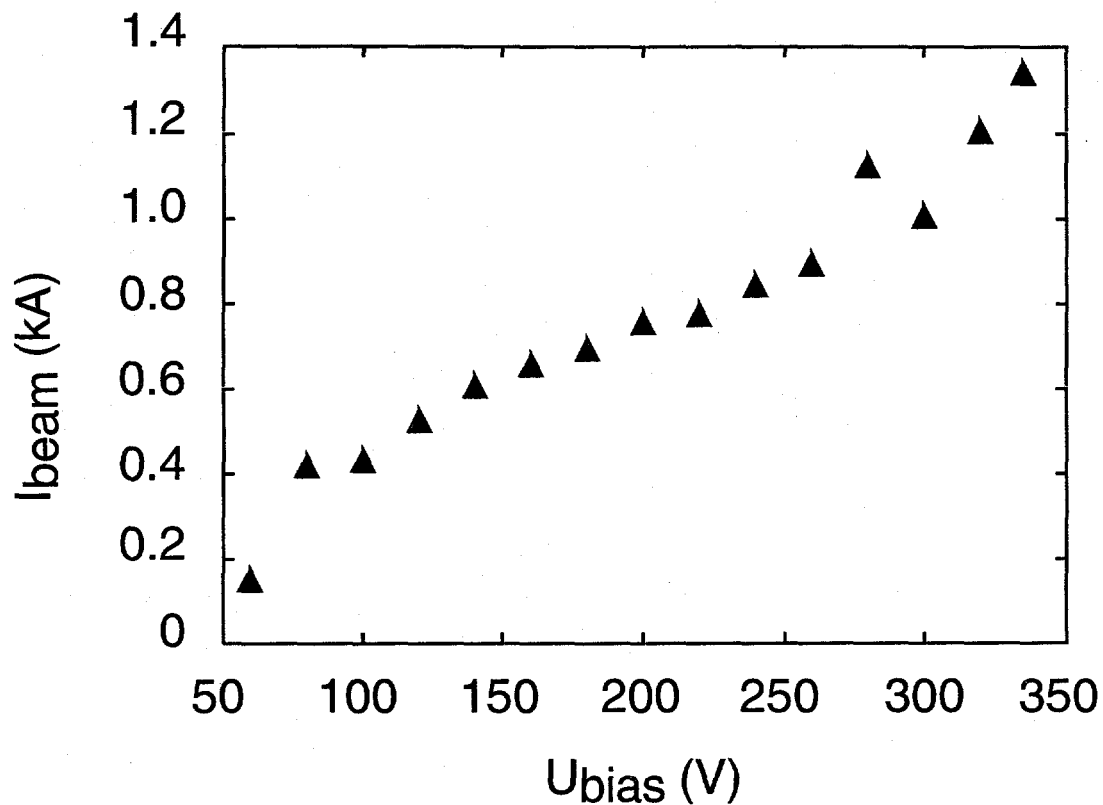


Fig. 7. Injected current I_{beam} vs. bias voltage U_{bias} at the discharge current $I_d = 1$ kA.

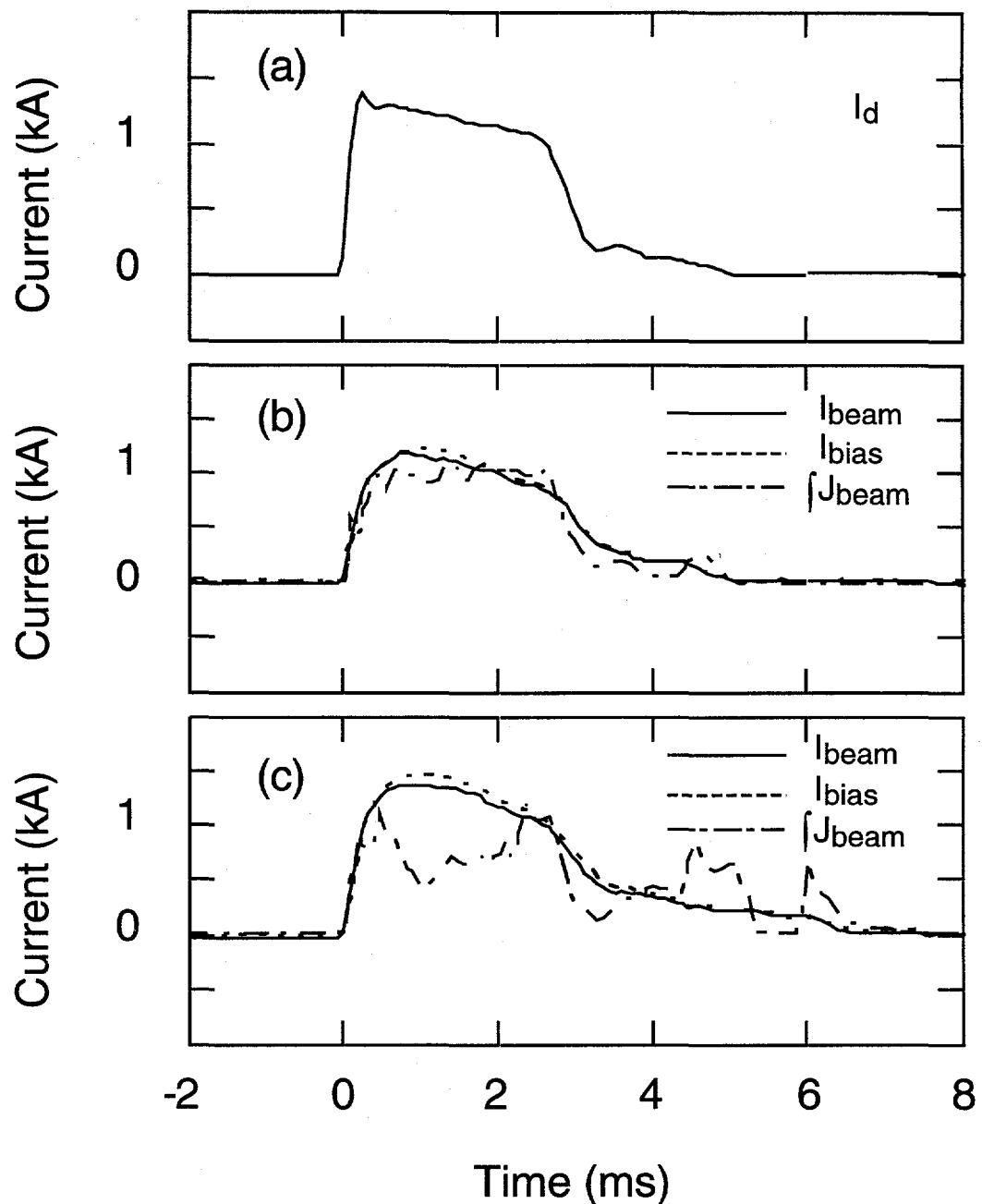


Fig. 8. Waveforms of the discharge current $I_d = 1.2$ kA, injected current I_{beam} , bias circuit current I_{bias} , and spatially integrated beam current density $\int J_{beam}$. The figure illustrated transition from (b) $I_{beam} < I_d$ to (c) $I_{beam} > I_d$.

4. Optimized Current Injector for MST

The geometry and the size of the current injector for MST is primarily dictated by the choice of access ports. It has been decided that the injectors will be inserted through the MST diagnostic ports which have a diameter of 3.8 cm (1.5"). Therefore, the outer diameter of the source was set at 3.7 cm and the discharge channel geometry was chosen to be that of type III. The cross-section of the injector is shown in Fig. 2.

The amplitude of the discharge current is limited by the duration of the plasma pulse. The current injection duration should be greater than the MST plasma energy confinement time which is a several milliseconds. On the other hand, the power deposition in the gun electrodes, allowed background pressure increase, and the pumping ability put an upper bound on the pulse length. As a compromise, the current injection duration was chosen to be 10 ms. Numerical simulations and experimental data extrapolation show that for a discharge time of 10 ms a discharge current of 1 kA is appropriate from the thermal load point of view. At this discharge current and duration the total amount of required hydrogen is $\sim 10^{19}$ molecules. Recall that during the injection the actual number of injected neutrals is probably lower due to a high degree of ionization.

The injector is enclosed in a boron nitride housing with an outer diameter of 3.7 cm and inserted through a port in the MST vessel. The position of the injector is normally 4 cm - 5 cm from the wall and the bias voltage is applied with respect to the vacuum vessel. In the experiments the injector was aligned parallel to the magnetic field, which was directed poloidally near the vessel wall. The injected current profile was measured with a miniature movable Rogowski coil situated at some distance (20 cm -

70 cm) from the gun in the poloidal direction and on the magnetic field line linking the gun. This experimental set-up is illustrated in Fig. 9.

(not to scale or accurate in detail)

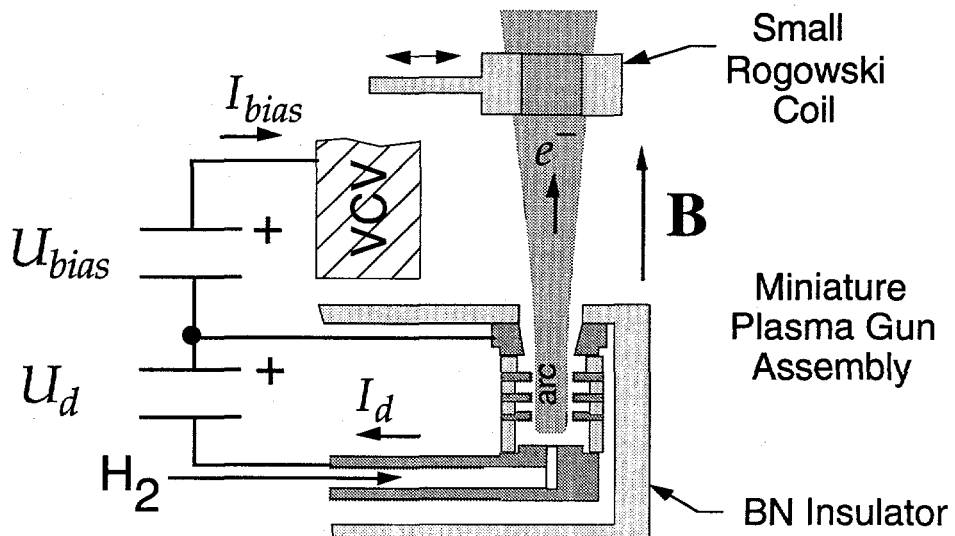


Fig. 9. Schematic of a typical plasma gun experiment in MST..

The waveform of the injected current is shown in Fig. 10. In this example, the gun plasma is formed 20 ms after the background MST plasma is initiated, and then V_{bias} is applied at 20.5 ms. Note that a limitation in the arc power supply allows only about 3 millisecond I_d pulse, but I_{bias} can be maintained much longer. We speculate that the internal discharge initiated by the arc power supply is not completely extinguished but rather is sustained to some degree through combined action of the bias power supply and the MST plasma. In general, the gun operates optimally when $I_d = I_{bias}$ which agrees with the optimization studied on the test stand. Without first

establishing the arc plasma, emission is irregular and not reproducible. Therefore, we plan to use a 10 ms arc power supply with a 10 ms bias power supply in our future injection experiments.

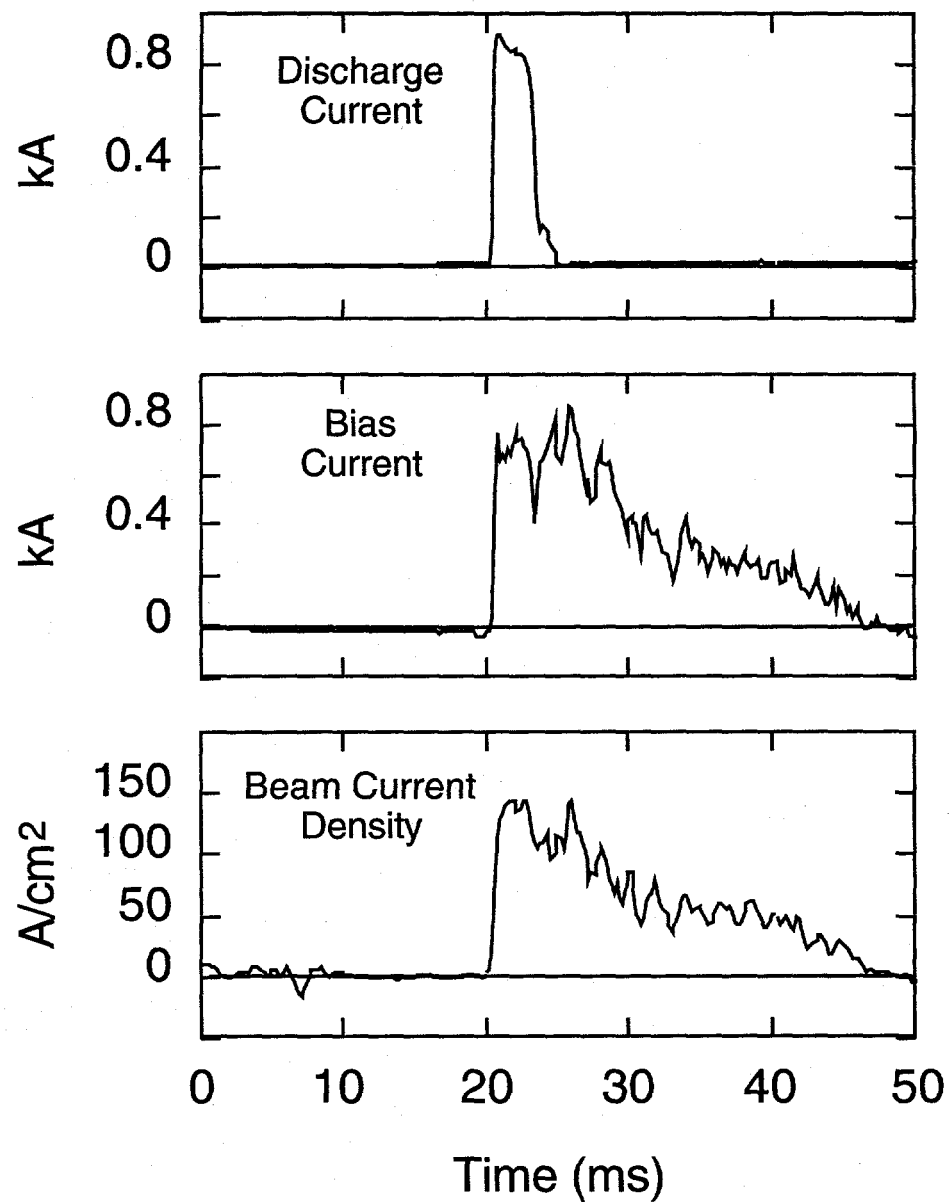


Fig. 10. Current injection in MST. Waveforms of the gun discharge current I_d , injected beam current I_{beam} and beam current density J_{beam} .

The injected current profile at a discharge current of 1 kA and a bias voltage of 270 V is shown in Fig. 11. The measured maximum emission current density is high (e.g., 100 A/cm² - 120 A/cm² at the peak) and the radial extent is about 3 cm. The profile integrated total current was about 1 kA which is about equal to the bias circuit current. This fact implies that the injected current has a high degree of directionality. The high directionality was also confirmed by rotating the gun 180°. Virtually all of the current emitted from the gun is observed in the "forward" direction as required for efficient current profile modification.

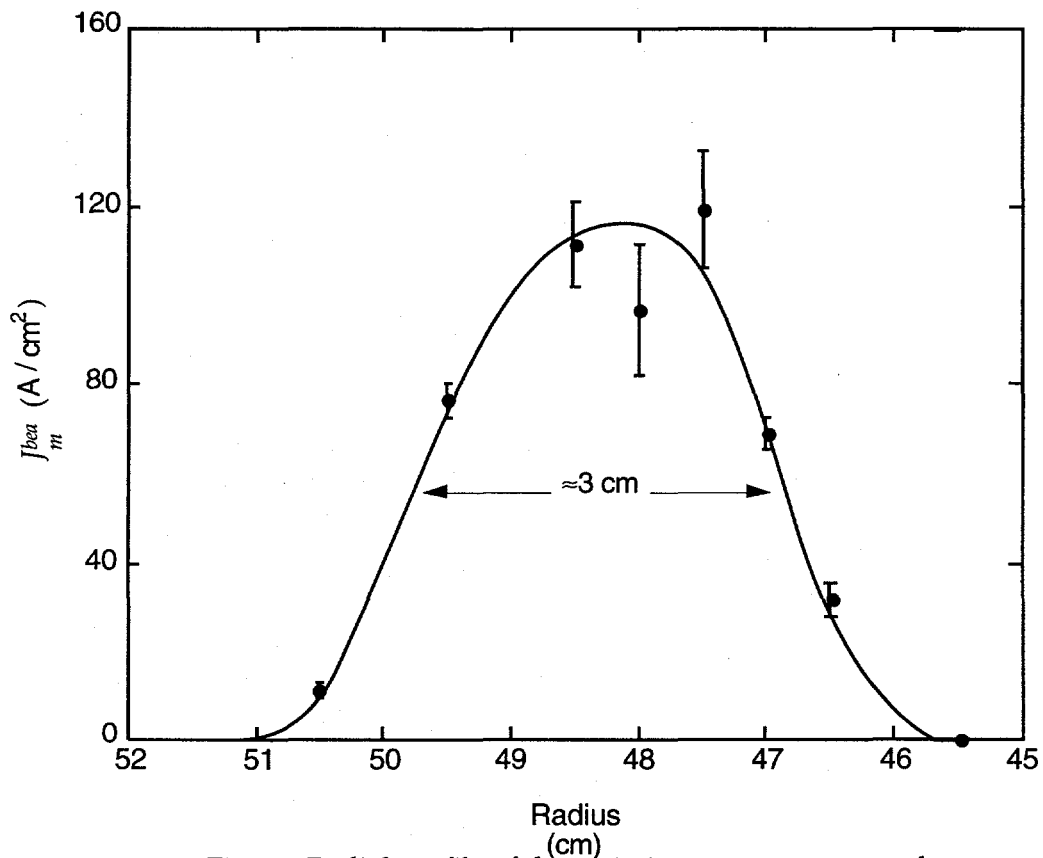


Fig. 11. Radial profile of the emission current measured with a movable Rogowski coil. The gun is located on the flux surface at 48 cm, separated from the Rogowski by 25 cm (poloidal angular separation of 30°). The total emission current is 1 kA, the arc current is 1 kA, and the emission bias voltage is 270 V.

The impurity generation was measured with the MST diagnostics which included monitoring of line intensities of impurities (C, O, Al) as well as the total radiated power. Previously tested metal electrode injectors generated a significant influx of impurities which sometimes terminated the MST plasma. We did not detect a change in the impurity level while operating the plasma injector. It appears that is that due to the high plasma density and temperature in the source the impurities are ionized and remain trapped in the plasma column. We are currently installing a VUV spectrometer for the diagnostics of Mo lines.

5. Conclusions.

We have developed a plasma electron injector for fusion and technological applications. The injector is based on a miniature plasma source and utilizes its plasma as an electron emitter. The nominal parameters of the injector are: size - 3.7 cm in diameter and 6 cm (not critical) in length, emission current - 1 kA, emission voltage - 250 V÷300 V, pulse duration - 10 ms, gas requirements - 10^{19} molecules/pulse.

The prototype source described in this paper will be replicated for the MST injection in order to attain this total current requirement of 20 kA. Each gun will have its own arc and emission power supplies providing a 10 ms injection pulse. The scope of technological application of the injector includes electron emitters, ion and electron beams, and plasma processing.

Acknowledgments:

The authors are grateful for the assistance of C.-S. Chiang, R. Kendrick, T.W. Lovell, S. Oliva, and M.A. Thomas.

This work was supported by the U.S. Department of Energy.

References

- 1 C.B. Forest et al., Phys. Rev. Lett. **68**, 3559 (1992).
- 2 R.J. Taylor, M.L. Brown, B.D. Fried, H. Grote, J.L. Liberati, G.J. Morales, and P. Pribyl, Phys. Rev. Lett. **63**, 2365 (1989).
- 3 R.J. Taylor and L. Oren, Phys. Rev. Lett. **42**, 446 (1979)
- 4 M.J. Schaffer et al., Bull. Am. Phy. Soc. **36**, 2325 (1991); E. J. Strait, Nucl. Fusion **21**, 943 (1981).
- 5 R.N. Dexter, D.W. Kerst, T.W. Lovell, S.C. Prager, and J.C. Sprott, Fusion Technology **19**, 131 (1991).
- 6 J.S. Sarff, A. F. Almagri, M. Cekic et al, Phys. Plasmas **2**, 2440 (1995).
- 7 G. Fiksel, S.C. Prager, W. Shen, and M.R. Stoneking, Phys.Rev. Lett. **72**, 1028 (1994).
- 8 M.R. Stoneking, S.A. Hokin, S.C. Prager, G. Fiksel, H. Ji, and D. Den Hartog, Phys.Rev. Lett. **73**, 549 (1994).
- 9 M. McGeogh, J. Appl. Phys. **71**, 1163 (1991).
- 10 T. Shibuya, S. Hashimoto, E. Yabe, and K. Takayama, Nucl. Instr. Meth. **B55**, 305 (1991).
- 11 Spectra-Mat, Inc. Catalog
- 12 G.I. Dimov and G.V. Roslyakov, Sov.Pribori Tech. Exp. **1**, 29 (1974)
- 13 G.Fiksel PhD Thesis, University of Wisconsin-Madison, 1991;
- 14 G. Fiksel, N. Hershkowitz, and M. Kishinevsky, Phys. Fluids B **3**, 834 (1991)

EXTERNAL DISTRIBUTION IN ADDITION TO UC-20

S.N. Rasband, Brigham Young University
T. Dolan, EG&G Idaho, Inc.
R.A. Moyer, General Atomics
J.B. Taylor, Institute for Fusion Studies, The University of Texas at Austin
E. Uchimoto, University of Montana
F.W. Perkins, PPPL
O. Ishihara, Texas Technical University
M.A. Abdou, University of California, Los Angeles
R.W. Conn, University of California, Los Angeles
P.E. Vandenplas, Association Euratom-Etat Belge, Belgium
Centro Brasileiro de Pesquisas Fisicas, Brazil
P. Sakanaka, Institute de Fisica-Unicamp, Brazil
Mme. Monique Bex, GANIL, France
J. Radet, CEN/CADARACHE, France
University of Ioannina, Greece
R. Andreani, Associazione EURATOM-ENEA sulla Fusione, Italy
Biblioteca, Istituto Gas Ionizzati, EURATOM-ENEA-CNR Association, Italy
Plasma section, Energy Fundamentals Division Electrotechnical Laboratory, Japan
Y. Kondoh, Gunma University, Kiryu, Gunma, Japan
H. Toyama, University of Tokyo, Japan
Z. Yoshida, University of Tokyo, Japan
FOM-Instituut voor Plasmafysica "Rijnhuizen," The Netherlands
Z. Ning, Academia Sinica, Peoples Republic of China
P. Yang, Shandong University, Peoples Republic of China
S. Zhu, University of Science & Technology of China, People's Republic of China
I.N. Bogatu, Institute of Atomic Physics, Romania
M.J. Alport, University of Natal, Durban, South Africa
R. Storer, The Flinders University of South Australia, South Australia
B. Lehnert, Royal Institute of Technology, Sweden
Librarian, CRPP, Ecole Polytechnique Federale de Lausanne, Switzerland
B. Alper, Culham Laboratory, UK
A. Newton, UK

2 for Chicago Operations Office
5 for individuals in Washington Offices

INTERNAL DISTRIBUTION IN ADDITION TO UC-20
80 for local group and file